This is a post-print version of a manuscript published in Forest Ecology and Management Volume 453, 1 December 2019, 117619
https://doi.org/10.1016/j.foreco.2019.117619

Preprint version of this manuscript is archived in bioRxiv
https://doi.org/10.1101/666305

High-resolution mapping of forest vulnerability to wind for disturbance-aware forestry

Authors and affiliations:

Susanne Suvanto*[1], Mikko Peltoniemi[1], Sakari Tuominen[1], Mikael Strandström[1], Aleksi Lehtonen[1]

[1] *Natural Resources Institute Finland (Luke), Latokartanonkaari 9, 00790 Helsinki*

***** *Corresponding author, susanne.suvanto@luke.fi*

Abstract

Windstorms cause major disturbances in European forests. Forest management can play a key role in making forests more persistent to disturbances. However, better information is needed to support decision making that effectively accounts for wind disturbances. Here we show how empirical probability models of wind damage, combined with existing spatial data sets, can be used to provide fine-scale spatial information about disturbance probability over large areas. First, we created stand-level damage probability models using wind damage observations within 5-year time window in national forest inventory data (NFI). Model predictors described forest characteristics, forest management history, 10-year return-rate of maximum wind speed, and soil, site and climate conditions. We tested three different methods for creating the damage probability models - generalized linear models (GLM[1]),

[1] ***Abbreviations:*** AUC – area under curve, BRT – boosted regression trees, dd – degree days, GAM – generalized additive model, GAMM – generalized additive mixed model, GIS – geographic information system, GLM – generalized linear model, GLMM – generalized linear mixed model, GTK – Geological Survey of Finland, GVIF – generalized variance inflation factor, MS-NFI – multi-source national forest inventory, NFI (NFI11, NFI12)

generalized additive models (GAM) and boosted regression trees (BRT). Then, damage probability maps were calculated by combining the models with GIS data sets representing the model predictors. Finally, we demonstrated the predictive performance of the damage probability maps with a large, independent test data of over 33,000 NFI plots, which shows that the maps are able to identify vulnerable forests also in new wind damage events, with area under curve value (AUC) > 0.7. Use of the more complex methods (GAM and BRT) was not found to improve the performance of the map compared to GLM, and therefore we prefer using the simpler GLM method that can be more easily interpreted. The map allows identification of vulnerable forest areas in high spatial resolution (16 m x 16 m), making it useful in assessing the vulnerability of individual forest stands when making management decisions. The map is also a powerful tool for communicating disturbance risks to forest owners and managers and it has the potential to steer forest management practices to a more disturbance-aware direction. Our study showed that in spite of the inherent stochasticity of the wind and damage phenomena at all spatial scales, it can be modelled with good accuracy across large spatial scales when existing ground and earth observation data sources are combined smartly. With improving data quality and availability, map-based risk assessments can be extended to other regions and other disturbance types.

Keywords: *forest disturbances; storm damage; windthrow; tree mortality; forest management*

1. Introduction

Forest wind disturbances have major economic, societal and ecological consequences in Europe. Forest disturbances have substantial effects on forest productivity and carbon storage (Seidl et al., 2014; Reyer et al., 2017). In European forests, the disturbance-related reduction of the carbon storage potential has been estimated to be 503.4 Tg C in years

– national forest inventory (11th Finnish NFI, 12th Finnish NFI), NLS – National Land Survey of Finland, RF-random forest, ROC – receiver operating characteristic

2021-2030 (Seidl et al., 2014). Actions to reduce and manage the disturbances are thus crucial in assuring the persistence of the forest carbon sinks. The damage caused by wind storms in European forests has increased during the past century (Schelhaas et al., 2003; Seidl et al., 2011, Gregow et al., 2017) and this trend is expected to continue (Ikonen et al., 2017; Seidl et al., 2017). The question of forest wind disturbances is therefore becoming increasingly important in the future.

Forest management practices play a key role in making forests less vulnerable to wind disturbances. Management driven changes in European forests, such as increasing standing timber volume and promotion of conifer species, have been identified as one of the major causes of increased forest disturbances in Europe during the latter half of the 20th century (Schelhaas et al., 2003; Seidl et al., 2011). If management practices are shifted to reduce forest vulnerability to wind, it may be possible to decrease the negative effects of wind disturbances. However, changing the forest management practises to more disturbance-aware direction is not always easy, as illustrated by the 2005 storm Gudrun in southern Sweden: despite the massive damage and economic losses caused by the storm and the Swedish Forest Agency's recommendations for alternative, less vulnerable, management options, the forest management practises in the area remained largely unchanged after the storm (Valinger et al., 2014, Andersson et al., 2018). This demonstrates that not only is information about the wind damage risks urgently needed to account for disturbances in management decisions, but it is also crucial that this information is in a form that can be effectively used and communicated to forest owners and managers.

The development of remote sensing methods and the progress of open data policies have substantially increased the amount, quality and availability of spatial data relating to forests. This opens new possibilities for detailed spatial estimation of forest sensitivity to disturbances. Vulnerability of forests to wind damage is affected by forest characteristics, forest management as well as the abiotic environment, such as local wind and soil conditions (Mitchell, 2013). For example, probability of wind damage has been shown to

78 increase with tree height and certain species, such as Norway spruce, are particularly
79 vulnerable to wind (Peltola et al., 1999; Dobbertin, 2002; Valinger and Fridman, 2011).
80 Forest management has major effects on wind damage sensitivity, as trees that have grown
81 in sheltered conditions and have later been exposed to wind, because of thinning or clear cut
82 of the neighboring stand, are especially sensitive to damage (Lohmander and Helles, 1987;
83 Peltola et al., 1999; Suvanto et al., 2016). Areas that are exposed to strong wind gusts
84 (Schindler et al., 2016) or where rooting conditions are limited due to soil characteristics
85 (Nicoll et al., 2006) are more predisposed to wind damage. Therefore, in order to provide
86 useful information on forest vulnerability to wind, information from several different sources,
87 scales and disciplines needs to be brought together.

88 Logistic generalized linear models (GLM) have long been applied in statistical modelling of
89 forest wind damage (Lohmander and Helles, 1987; Valinger and Fridman, 1997; Suvanto et
90 al., 2016). In addition, different approaches allowing more flexible model behaviour than fully
91 parametric GLMs have been used, such as generalized additive models (GAM; Schmidt et
92 al., 2010) that use non-parametric smooth functions to allow more flexibility in the
93 relationship of response variable and predictors (Hastie et al., 2009). Machine learning
94 approaches have also been successfully applied to wind disturbance modeling (see
95 Hanewinkel et al. 2004 for an early example) and recently especially tree-based ensemble
96 models, such as random forests (RF) and boosted regression trees (BRT), have been
97 popular and often shown to perform well in predicting wind damage (see Schindler et al.,
98 2016; Kabir et al., 2018; Albrecht et al., 2019; Hart et al., 2019 for examples using RF and
99 Díaz-Yáñez et al. 2019 for BRT). While machine learning methods and additive models are
100 able to more flexibly fit the data and account for non-linearities, GLMs have strengths in their
101 straightforward interpretability and the robustness of predictions (Nakou et al., 2016;
102 Albrecht et al., 2019).

103 In this study, our goal was to answer the need for information to be used for taking forest
104 disturbances into account in management decisions by creating a high-resolution map of

forest vulnerability to wind damage, using damage observations from national forest inventory (NFI) data. While there have been some previous attempts to map forest vulnerability to wind damage using statistical models (Schindler et al., 2009; Saarinen et al., 2016; Suvanto et al., 2016), the resulting maps and their applicability to disturbance situations outside of the original model data have rarely been rigorously tested, limiting the conclusions that can be drawn about the performance and usefulness of such maps. In addition, we aimed to test the suitability of different modelling methods, ranging from fully-parametric GLM to more flexible methods, for creating such maps. More specifically, our aims were to (1) create a damage probability statistical model based on a large and representative data set of wind damage observations in the Finnish NFI, (2) compare three methods for creating the model, GLM, GAM and BRT, to test the suitability of different methods for the task, (3) calculate a damage probability maps by combining the models with national extent GIS layers of model predictors, compiled from different sources, and (4) test the performance of the maps with a large data set containing independent damage observations from over 33,000 NFI plots.

2. Material and methods

2.1 National Forest Inventory and wind damage observations

In this study, we used stand level wind damage observations from the 11th Finnish national forest inventory (NFI11) to create an empirical model of wind damage probability (Fig. 1). The field work for the NFI11 was conducted from 2009 to 2013 (Korhonen, 2016; Korhonen et al., 2017). In later stages of the study, we also used NFI12 (field work in 2014 to 2018) to test the created map (see section 2.5).

In our analysis, we only included plots that were defined as forest land. Poorly productive forests were excluded because they are unimportant for forestry and their wind damage risks tend to be small due to low volume of growing stock. In addition, plots on treeless stands or seedling stands without upper canopy layer were excluded because seedlings have very low

wind damage probability (8633 plots). Plots with missing data or unrealistic (erroneous) values for any of the used variables were excluded (52 plots). Plots within less than 1 km from the national border were also excluded, as the data set describing local wind conditions (Venäläinen et al., 2017) had edge effects (214 plots). If a plot was located on the border of two or more forest stands, we only used the data from the stand where the plot centre was located. The final data set consisted of a total of 41,392 NFI plots.

Observations of stand level wind damage and an estimate of the damage time is documented in the Finnish NFI (Tomppo et al., 2011; Korhonen, 2016). Here, we used only the wind damage observations that had occurred no more than 5 years before the date of the field visit. Since the field work of NFI11 was done in 2009 to 2013, the data can contain observations from damage that has occurred between 2004 and 2013. During these years, several high impact storms affected Finland, such as cyclone Dagmar (known as Tapani in Finland), which caused severe damage in Finland during December 26th and 27th 2011 (Kufeoglu and Lehtonen 2014), and a series of severe thunderstorms in summer 2010 (Viiri et al. 2010).

The severity of damage was not considered in the analysis, because the degree of damage was only recorded as cumulative effect of all damage agents, and no information of wind damage severity was available in cases where there was more than one damaging agent present. The restriction of the analysis to only severe damage cases would also have limited the number of damage observations available. Therefore, the binary damage variable contains stands with different damage severities. Stand level wind damage was observed at 1,070 plots of the total 41,392 NFI plots in the dataset.

2.2 Model predictors

2.2.1 National Forest Inventory data

Most predictors in the statistical models were extracted from the NFI field data (Tables 1-2). To describe the forest characteristics of the stand, dominant tree species and mean tree

height in the stand were used. If several canopy layers and species were recorded in the data, the values from the layer with largest tree height were used, as the tallest trees can be assumed to be most vulnerable to wind. The NFI also documents the type and time of most recent forest management operations, and based on this data we created a variable describing the time since last thinning.

NFI information about soil type, soil depth and site fertility was also used (Tables 1-2). Soil type variable differentiated between organic and mineral soils, as well as fine and coarse grained mineral soils. Fine mineral soils included clay and fine sands, whereas sands and coarser soils were classified as coarse mineral soils. Grain size was estimated on the field by NFI teams. Site fertility classes in the NFI are estimated in eight classes, but in our analysis they were regrouped into two classes so that class “Fertile” contained sites from herb-rich to mesic forests on mineral soils and from euthrophic to meso-oligothrophic peatlands. Less fertile classes were included in the “Poor” fertility class (see Tomppo et al., 2011 for detailed description of the site fertility classes used in the Finnish NFI).

The used data covers the whole country and contains damage observations from several years and, there is thus large variation in the wind conditions experienced by the trees in the data. Not all plots were exposed to similar wind conditions and this needed to be taken into account in the statistical model. However, we did not have reliable data available about the spatial variation in maximum wind speed conditions during the study period and lacking such an important factor affecting the damage probability is likely to bias the estimation of the effects of other predictors. Therefore, a different approach was taken. To account for areas subjected to severe storm events, variable “Damage density ratio” was calculated using the locations of NFI plots as the ratio of 2D kernel density of damaged plots and all plots (Table 1). That is, the ratio describes the spatial density of damaged plots in comparison to all NFI plots included in the model. A value of 2, for example, can therefore be interpreted as two times higher density of damaged plots than what would be expected from the density of all plots. The damage density variable was then transformed into a categorical variable (with

classes 0-2, 2-3, and >3). The upper limit of the lowest class was set relatively high to identify only the strongest clusters of damaged plots and to avoid catching all the large-scale spatial trends with this variable. The calculations were done in R with the *KernSmooth* package (Wand, 2015) using bandwidth of 20 km (see details in S1).

2.2.2 Other data sets and the delineation of forest stands

In addition to the NFI field data we also supplemented the model predictor set with additional variables describing local wind conditions and open forest borders from other data sources (Tables 1-2). To describe the long-term wind conditions at each plot, we used a data set describing the local 10-year return levels of maximum wind speeds in 20 m x 20 m raster cells. That is, the value of each pixel represents the level of maximum wind speed (ms^{-1}) expected to be reached on average once in every 10 years (detailed description of the data and its methodology in Venäläinen et al., 2017; see S5 for map of the data). The data is downscaled from coarse-scale wind speed estimates in ERA-Interim reanalyzed data with a wind multiplier approach using CORINE land-use data and digital elevation model (Venäläinen et al., 2017). The data set contains maximum wind speeds calculated for eight different wind directions, and in this study we used the maximum value of these for each pixel.

To identify stands with open forest borders (variable 'Open neighbour stand', Table 1), we used the multi-source NFI forest resource maps (MS-NFI; Tomppo et al., 2008; Mäkisara et al., 2016) that combine satellite data and NFI field data to create national extent forest resource maps in a 16 m x 16 m resolution grid.

However, the used wind damage observations were documented on the level of forest stands and the stand borders were not mapped in the data but only estimated by the NFI team at the field. Therefore, in order to combine the stand-level damage information with other data sources, the locations of stand borders first needed to be defined. A forest stand in the the Finnish NFI is defined as spatially continuous land area that is homogeneous with

respect to properties such as administrative boundaries, site fertility, structure of the growing stock (e.g. maturity class, tree species composition) and forest management (Tomppo et al., 2011). To create polygons that would approximately correspond to the stands assessed in the field by the NFI team, we used image segmentation on the MS-NFI data layers (corresponding to year 2013) describing growing stock volumes by main tree species groups (pine, spruce and deciduous species) and tree height. Land property boundaries obtained from the National Land Survey of Finland were also included in the segmentation, as they are considered as stand boundaries in the NFI. The image segmentation was conducted with the methodology described by Pekkarinen (2002), using the "segmentation by directed trees" algorithm by Narendra and Goldberg (1980).

Once the stand polygons were defined with image segmentation, they were used for calculating local wind conditions and finding stands with open stand borders. For each stand polygon, maximum wind-speed within the stand boundaries was calculated (Table 1). Maximum value was used because the NFI field data does not specify the exact location of the damage within the stand, and we assumed that damage occurred in the most wind exposed part of the stand.

To identify plots with open neighbor stands, median tree height was first calculated for each stand polygon using the MS-NFI tree height data. A stand was defined to have an open stand neighbor if the median tree height of any of the stand neighbours was smaller than 5 meters (Table 1). Median was used instead of mean so that it would be less affected by possible outlier values resulting from inaccuracies in defining the stand polygons.

Calculations of maximum wind speeds and open stand neighbors for the segments were conducted with PostGIS (version 2.4.0) and Python (version 2.7.12) with packages *geopandas* (version 0.3.0) and *rasterstats* (version 0.12.0).

2.3 Statistical modelling

Damage probability models were created using three different methods: GLM, GAM (Wood 2006) and BRT (Elith et al., 2008). In all the models the dependent variable was the presence of wind damage in the stand and independent variables described forest characteristics, forest management history, soil and site type, the 10-year return level of maximum wind speed, temperature sum and the local damage density ratio (Table 1).

Binomial GLM with logit-link function were fitted in R (version 3.5.1, R Core Team, 2017). To account for non-linear relationships, logarithm transformation were tested for all continuous independent variables and included in the final model if they showed lower AIC than models with non-transformed variables. The transformations were included only for the GLM model, since GAM and BRT enable more flexibility in the shapes of the relationship between response variable and predictors, and can therefore account for non-linear relationships without transformations.

Variable selection was based on several criteria: (1) only variables that, based on earlier research, were expected to have a causal effect to wind damage probability were included, (2) since the ultimate goal of the model was to produce the damage probability map, we only included variables for which reasonably high-quality national-extent GIS data sets were available or could be derived from existing data, (3) the behaviour of the variable in the model was plausible based on existing understanding of forest wind damage. We also aimed to build the model so that all major components related to wind damage probability were included. Collinearity of predictors was inspected with Pearson's correlation coefficients and generalized variance inflation factors (GVIF, Fox and Monette, 1992). All correlations between included continuous predictor variables were weaker than 0.5 and GVIFs for all variables were lower than 4.

GAM is an extension of a GLM where the linear predictor contains a sum of smooth functions of covariates. This specification of the model in terms of smooth functions instead of detailed parametric relationships allows for more flexibility in the dependence of the

response of the covariates (Wood, 2017). In our analysis, GAM with logit-link function was fitted in R with package *mgcv* (version 1.8-24, Wood, 2011), using the same predictors that were included in the GLM. All continuous predictors were included in the model through non-linear smoothing spline functions. The dimension parameter (k), effectively setting the upper limit on the degrees of freedom related to the smooth, was set to 15 for all variables, except for temperature sum for which k = 5 was chosen to avoid unrealistically fluctuating large-scale patterns in the predictions. The effective degrees of freedom (edf) after fitting the model were lower than k for all of the terms (see S2 for details), suggesting that the chosen k's were sufficiently large.

BRT is an ensemble method that combines a large number of regression trees with a boosting algorithm (Elith et al., 2008). Here, BRTs were computed with R package *dismo* (version 1.1-4, Hijmans et al., 2017). To find the best parameters, BRTs with different parameter combinations of tree complexity (tested values 1, 2, 3 and 5), learning rate (0.05, 0.01 and 0.005) and bag fraction (0.5, 0.6 and 0.75) were fitted. The number of trees was not assigned manually, but was estimated with k-fold cross-validation using the function *gbm.step* (Hijmans et al., 2017). To estimate the number of trees and to compare different parameter combinations, *gbm.step* was run separately for each parameter combination. Following the rule-of-thumb suggested by Elith et al. (2008), we excluded parameter combinations that led to models with fewer than 1000 trees. Thus, the model with parameter combination leading to lowest holdout residual deviance in the cross-validation performed by *gbm.step* and at least 1,000 trees was chosen for the final model (tree complexity = 2, learning rate = 0.01, bag fraction = 0.5, 2,250 trees, see S3 for details).

To make sure that the unbalanced ratio of damaged versus non-damaged plots did not affect the results, BRTs were fitted also from two balanced datasets where the balancing of the observations was done by (1) undersampling the non-damaged plots or (2) oversampling the damaged plots. In both cases the cross-validated area under curve (AUC) values were very

similar to ones calculated from the original unbalanced dataset and, therefore, the original data set was used for the final results.

To account for the sampling design, weights based on the forest area each plot represents were used in all models (Korhonen, 2016). For example, in northern Finland the NFI sampling design is sparser and therefore the weight of one plot in modelling is higher. To test if the clustered sampling design had an effect on the results, GLMs and GAMs were also fitted as mixed models (GLMM and GAMM) with plot clusters as random intercepts, using R packages lme4 (Bates et al., 2015) for GLMM and gamm4 (Wood and Scheipl, 2017) for GAMM. However, as the mixed model predictions (in the scale of the linear predictor, using only fixed effects for prediction) were highly correlated with the fixed effect model prediction (Pearson's $r = 0.998$, $p < 0.001$ for GLM vs GLMM, and $r = 0.979$, $p < 0.001$ for GAM vs GAMM) and our interest was in marginal instead of conditional inference, no random effects were included in the final models.

The models were validated with 10-fold stratified cross-validation, where number of damaged plots was divided evenly into the folds. In the cross-validation, the variation in damage density variable was not used in the prediction, because the variable was included in the model only to account for spatial structures in storm severity in the data, and in an aimed use case of the models (i.e., estimating damage vulnerability in future events) we would not have this information available. Instead, separate predictions for test-folds were calculated with each class of the damage density variable (0-2, 2-3, >3). Then, these three predictions were averaged based on the frequency of each class in the original model data. See details in S1.

Receiver operating characteristic (ROC) curves and AUC values were calculated for each iteration of cross-validation and used to assess the performance of the models. The ROC curve plots the true positive rate (sensitivity) and true negative rate (specificity) of the model with all possible classification thresholds. The AUC values represent the area under ROC

curve and measure the model's ability to discriminate between events and non-events. AUC values of 0.5 correspond to a situation where the classifier is no better than random (ROC curve along diagonal) and value of 1 a situation where the model perfectly discriminates between events and non-events. As a rule of thumb, AUC values over 0.7 are considered acceptable discrimination between classes, values over 0.8 excellent and values over 0.9 outstanding (Hosmer et al., 2013).

2.4 Calculation of the damage probability map

A GIS raster data layer with resolution of 16 m x 16 m and extent of the whole country was prepared for each predictor variable used in the models (Table 1). Forest variables (dominant species, tree height, height-diameter ratio, open forest edge) were derived from the Finnish MS-NFI data for year 2015 (Mäkisara et al., 2019). A grid cell was defined to be on an open forest edge if tree height in the MS-NFI data was lower than 5 meters in any of the cells within a 5 x 5 cell neighborhood.

Spatial data on forest management history (the time of last thinning) was derived from the forest use notification collected by the Finnish Forest Centre. This data consists of forest use notifications that forest owners are required to report to the Forest Centre before conducting management operations in their forests. For each 16 m x 16 m pixel, we first assigned the year of the latest notification of planned thinning in that location of the pixel and then calculated the difference to year 2015.

Data for the 10-year return-rates of maximum wind (Venäläinen et al., 2017), originally in 20 m x 20 m resolution, was resampled to the 16 m x 16 m grid with GDAL using bilinear interpolation. Soil type was defined as ORGANIC for areas within the peatland polygons in the Topographic Database produced by the National Land Survey of Finland (NLS, 2018). Other areas were defined as mineral soils, and further divided to fine or coarse mineral soils based on the top soil information in the 1:200,000 resolution soil map of the Geological Survey of Finland (GTK, 2018). Data layer for soil fertility classes was made by reclassifying

339 the MS-NFI fertility class data layer from the original five classes to the two classes used in
340 the models (see details in section 2.2.1). Average annual temperature sum was calculated
341 with a threshold of 5°C from daily weather data grids (Aalto et al., 2016) for the years 1985
342 to 2014.

343 Similarly as in the cross-validation, the variation in damage density variable was not used in
344 the prediction, because we would not have this information available for future events.
345 Instead, separate predictions were calculated with each class of the damage density variable
346 and these three predictions were then averaged based on the frequency of each class in the
347 original model data. See details in S1.

348 The damage probability map was calculated from the GLM, GAM and BRT model objects
349 and the GIS data layers using R packages *raster* (Hijmans, 2017) and *sp* (Pebesma and
350 Bivand, 2005).

351 2.5 Testing the map with new damage observations

352 The accuracy of the damage probability map was validated with an independent test data
353 set. The map was compared to the damage observations in the most recent NFI
354 measurements (12th Finnish NFI, NFI12), which were not included in the model fitting data
355 that was from the NFI11. Compared to NFI11, which covers the whole country, NFI12 does
356 not cover the northernmost parts of Finland as plots in the three most northern municipalities
357 (Northern Lapland), where the proportion of forest land is low, are not measured as
358 frequently as other parts of the country (see S5 for maps of plot locations in NFI11 and
359 NFI12).

360 We included the NFI12 plots that had been measured during 2014-2018, were classified as
361 forest land by the field team, and were located within forest area in the MS-NFI forest
362 resource maps (i.e., there were data in the wind damage probability map at the location of
363 the plot). For wind damage we also used the same criteria as with the model data, i.e. only
364 observations estimated to have occurred during the last 5 years were included and the

severity of the damage was not considered. In addition, those permanent plots that were measured already in NFI11 were excluded from the test data, as the previous measurements in the same plots were used in the model fitting. The final test data consisted of 33,754 plots with wind damage in 734 of the plots.

Values of the wind damage probability maps were extracted at the locations of test data plots as the mean value of map pixels within 20 meter buffer from the location of the plot center. ROC curves and AUC values were calculated using the wind damage information in the test data and the extracted values of the damage probability maps. The extraction was conducted in R with package *raster* (version 2.8-19, Hijmans, 2017) and ROC/AUC calculations with package *pROC* (version 1.12.1, Robin et al., 2011).

3. Results

The results showed that forest vulnerability to wind damage is strongly driven by forest characteristics, especially tree height. In all models, the damage probability increased with tree height, and the increase was strongest for spruce dominated forests (see Fig. 2 and Table 3 for GLM, Fig. 3 for GAM and Fig. 4 for BRT). Higher values of damage density ratio led to higher damage probability in all models, as expected (Fig. 5). Also forest management affected damage probability in the models, as recently thinned forests and forests with open stand borders were more susceptible to damage. These predictors, related to the forest characteristics, very much drive the fine-scale spatial variation of damage probability in the (Fig. 7).

Wind damage probability was found to show distinct large-scale trends, most importantly the decreasing damage probability from south to north (Fig. 7). This effect in the models comes from the temperature sum, but also other predictors contributed to the large-scale trends in the map, as there as large-scale patterns in wind conditions, forest characteristics and soil and site fertility conditions (see Fig. 2 for GLM, Fig. 3 for GAM and Fig. 4 for BRT, S5 for maps of predictor raster data). The north-south pattern in damage density was evident in the

391 damage probability maps with all model methods. However, the map created with the BRT
392 showed unexpectedly high damage probability values for the northernmost parts of the
393 country (Fig. 7).

394 The model predictors showed in general rather similar effects in the three tested methods
395 (GLM, GAM and BRT). Yet, there are also differences, especially in the shape of relationship
396 between the continuous predictors and predicted damage probability. In GLM, the
397 relationships are restricted to sigmoidal curves (Fig. 2), whereas GAM (Fig. 3) and BRT (Fig.
398 4) allow more flexible shapes of responses. This can be seen, for example, in how
399 increasing tree height in pine forests shows steadily increasing damage probability with GLM
400 (Fig. 2) whereas in GAM damage probability peaks around tree height 200 dm and then
401 declines (Fig. 3).

402 As the BRT predictions are calculated from ensembles of regression trees, they enable very
403 sharp changes in the prediction within small changes in the values of the predictor (Fig. 4).
404 They can also contain diverse interactions between the predictors, which are unfortunately
405 not visible in partial dependence plots like Fig. 4. The BRT results showed somewhat
406 different trends than the other methods in model responses to predictors (Fig. 4). For
407 example, while tree height in spruce forests increases damage probability throughout the
408 range of data in GLM (Fig. 2) and GAM results (Fig. 3), in BRT results similar strongly
409 increasing trend is not found, instead the relationship between height and damage
410 probability seems to saturate for all tree species (Fig. 4). The large-scale spatial patterns in
411 map prediction also differed for BRT compared to the other models, as high values of
412 damage probability were predicted for the northernmost parts of the country. (Fig. 7).

413 Cross-validation showed higher predictive performance of the GAM model compared to the
414 GLM and BRT (Fig. 6). However, when the final damage probability maps were tested with
415 the NFI12 test data, all models showed very similar performance in discriminating between
416 damaged and non-damaged plots in the test data. (Fig. 8). All maps gave on average higher

damage probability values for damaged than non-damaged plots and showed an acceptable level of discrimination between the two (AUC > 0.7). The added flexibility and ability to account for nonlinear relationships in GAM and BRT did not considerably improve the predictive performance of maps compared to the fully parametric GLM (Fig. 8).

4. Discussion

4.1 The damage probability map

We created a new spatial wind damage risk product based on inventory data spanning over several years and several other data spatial sources, including information where the actual harvests have recently occurred in Finland. Validation of the map with independent and large data set showed that the map is able to identify vulnerable stands also in new storm events. While there have been attempts to map wind damage probability based on empirical damage models (Schindler et al., 2009; Saarinen et al., 2016; Suvanto et al., 2016), our work here uniquely provides national extent and high spatial resolution information about forest vulnerability to wind and its validity is also tested with large external test data.

The successful identification of damage vulnerability in an independent test data is not trivial. First of all, wind damage is challenging to predict and extending the performance of statistical wind damage models to new data sets has been shown not to be straightforward (Fridman and Valinger, 1998; Lanquaye-Opoku and Mitchell, 2005; Kamimura et al., 2015). Moreover, because we wanted to test how well our map identifies forest vulnerability to wind in future events, for which we don't have detailed information of, we did not include any information about spatial distribution of wind speeds or storm events during the time frame of the test data when we tested the map. Thus, the discrimination of damaged from non-damaged plots with fair accuracy (AUC = 0.726) for the entire extent of Finland indicates that the map is indeed successful in identifying the vulnerable forests, and implies that efficient combination of inventory data and several new spatial data sources is a promising way to map damage risks.

443 A major factor contributing to the successful extension of the map to new test data was the
444 large and systematically sampled forest and damage data that spanned over several years.
445 Thus, our model was able to represent the different conditions (forest characteristics, soil,
446 etc.) within the country. The need for comprehensive model data in empirical wind damage
447 models has been demonstrated, for example, by Hart et al. (2019) who showed that it is
448 possible to generalize to new storm events when the model data covers the variation of
449 predictor variables in the new data set.

450 In addition to good representation of environmental and forest conditions, our data also
451 represents different types of wind events, since the data consisted of damage observations
452 in a 5-year time window. Most wind disturbance studies typically concentrate on one or few
453 storms (e.g., Schindler et al., 2009; Kamimura et al., 2015; Saarinen et al., 2016; Suvanto et
454 al., 2016; Hart et al., 2019), which limits their ability to generalize to different storm events.
455 While modelling of multi-event data can be more challenging than single-event data
456 (Albrecht et al., 2019), we argue that it is necessary when the purpose of the model is in
457 assessing damage probability in new storm events, outside of the original model data.

458 Availability of high-quality and high-resolution spatial data of the model predictors was also
459 crucial for the ability of the damage probability map to identify damaged stands in the test
460 data. Additional uncertainties arise from the input data sets when model predictions are
461 made with GIS data gathered from several different sources instead of the field-measured
462 data that were used for fitting the model. In our case, we were able to utilize several high-
463 quality and high-resolution data sources, such as the MS-NFI raster maps of forest
464 characteristics (Mäkisara et al., 2019) and new data products of local wind conditions
465 (Venäläinen et al., 2017). We were also able to use the recently opened forest use
466 notification data from the Finnish Forest Centre that provided us with nation-wide information
467 about the recent forest management history of the stands. This type of legacy information
468 about forest management is typically difficult to obtain and has rarely been included in
469 predictive wind damage risk models before, despite the clear effects of management history

on forest disturbance dynamics. While all these data sources contain uncertainties, the verification of our map with independent test data showed that they were nevertheless able to represent well the main factors determining forest susceptibility to wind.

With new data sources and increasing quality and availability of data in the future, the accuracy of the map could still be improved. This could mean, for example, improved accuracy of tree height information through the use of lidar data or inclusion of variables that were left out of the current map due to lack of national level spatial data about their distribution (e.g. distribution of wood decaying fungi that weaken trees' resistance to wind). Soil data had maybe the lowest resolution and higher uncertainties of the used GIS data and, therefore, increased quality of those data sets would also be desirable. However, the effects of soil variables in the model were relatively small, and therefore the effects of only improving the soil GIS data in the prediction would most likely not be drastic. Instead, more detailed soil data would be needed for the model data to improve the description of the role of soil characteristics on tree vulnerability to wind in the model. Integrating projections of future wind climate would also add value to the map, as the current version only uses data describing present wind conditions (that is, the data by Venäläinen et al. 2017).

4.2 Drivers of forest susceptibility to wind disturbance

The factors that were found to affect damage probability in our results are well in line with previously published results. For example, increasing damage probability with tree height and the higher vulnerability of Norway spruce have been shown in previous studies (Peltola et al., 1999; Valinger and Fridman, 2011; Suvanto et al., 2016). New stand edges after clearcutting of the neighboring stand and recently thinned stands have also been known to be at higher risk of windthrow (Lohmander and Helles, 1987; Peltola et al., 1999; Wallentin and Nilsson, 2014).

While open stand edges did increase the risk of wind damage in our results, the effect was not as distinct as could be expected from earlier research that emphasizes the role of forest

edges (e.g., Peltola et al., 1999). This may in part result from the use of stand level data, where defining and identifying the open stand borders from the NFI data is more uncertain than in the case of tree-level analysis (see section 2.3.2 for the used methodology). Earlier work with storm damage data from severe autumn storms in Finland showed that the effects of open forest edges on damage probability were more emphasized in tree-level analysis (Suvanto et al., 2018) than in the stand-level analysis of the same data (Suvanto et al., 2016). In the future, potential improvements to the presentation of damage probability at the forest edges in the map could be achieved by combining tree-level results or mechanistic approaches to the current stand-level modeling approach.

In the model, the effect of wind speed data (Venäläinen et al., 2017) on damage probability showed logical behaviour of increasing damage probability with increasing 10-year return-rates of maximum wind speed. The wind speed data accounts for the effects of topography on general wind conditions, and therefore variables describing topographical conditions were not included in our models, even though they have been shown to be linked with wind damage probability (e.g., Schindler et al., 2009).

Variation in wind conditions were accounted for in the models by two variables: 10-year maximum wind speed return-rates, which described the local long-term wind conditions at the plots, and the damage density variable, which was used to account for major storm events during the study period due to the lack of direct wind speed data with sufficient spatial coverage and accuracy. The use of indirect variable (damage density) to account for this has the risk of not representing the occurred wind conditions well enough, and thus distorting the estimates of other predictors. However, in our results the damage density variable seems to have filled its purpose, as the relationships between predictors and damage density are well in line with previous research and the maps resulting from the models are able to identify the vulnerable stands also in the test data, in which the plots have been affected by different storm events.

Large-scale geographical patterns in our results showed that the probability of wind damage in Finland decreases from south to north. This is in agreement with results from previous studies combining forest model simulations with mechanistic wind damage models (Peltola et al., 2010; Ikonen et al., 2017). The higher susceptibility of forests in southern Finland to wind disturbances is related to the shorter length of the soil frost period in southern parts of the country. When the soil is frozen, trees are well anchored to the ground and less vulnerable to windthrow and, therefore, forests located in areas with longer periods of soil frost are less likely to be damaged during winter storms (Gregow et al., 2011; Laapas et al., 2019). However, other factors affecting forest wind susceptibility also change along the north-south gradient. The proportion of Scots pine, a species more resistant to wind than Norway spruce, increases towards north, and trees in the north have on average lower height-to-diameter ratio, which is linked to wind damage sensitivity (Peltola et al., 2010; Ikonen et al., 2017). In addition, in southern parts of the country, forest stands are smaller in area and there are less protected areas compared to the north. Thus, more frequent windthrows related to new stand edges and recent thinnings may also contribute to higher damage probability in the south. Similarly, butt rot caused by *Heterobasidion* sp., which increases tree vulnerability to wind (Honkaniemi et al., 2017), currently affects the southern parts of the country more severely (Mattila and Nuutinen, 2007; Müller et al., 2018) and may also contribute to the north-south pattern in the wind damage probability in our results. Therefore, it is not entirely clear what are the exact mechanisms causing increased damage probability with temperature sum in our model.

4.3 Comparison of methods

While the results for GLM and GAM models were rather similar, the BRT showed somewhat different model behaviour in the responses of damage probability to the predictors (Fig. 4) and different patterns in the spatial prediction (Fig. 7). Since the visible differences in the predictions are in the northernmost part of the country, the lack of test data in this area (see S5) makes the interpretation of the test results (Fig. 8) for the BRT challenging, as the area

549 with unexpected BRT predictions is mainly not covered by the test data. In any case, the
550 high values of BRT predictions in northernmost Finland do not seem realistic.

551 Our results did not show improved predictive performance of the map with the more flexible
552 methods, GAM and BRT, compared to the logistic regression model (GLM). This is
553 somewhat surprising, especially in the case of BRTs, as they are able to account for non-
554 linearity and interactions between predictors flexibly and this has been seen as an
555 advantage leading to more accurate predictions (Elith et al. 2006, 2008, Díaz-Yáñes et al.
556 2019). It seems that while BRT has advantages in accounting for more complex
557 relationships and interactions in the data, they may also catch patterns that are not helpful
558 for making predictions for test data (see, e.g., the unrealisticly high probabilities of damage
559 with very low wind speeds in BRT, Fig. 4). This is likely to hamper the performance of BRTs
560 in our study so that they are not able to improve cross-validation performance compared to
561 GLM.

562 While Díaz-Yáñes et al. (2019) used BRTs for modelling wind and snow data using NFI data,
563 they unfortunately did not compare the method to other methods, report metrics about how
564 well the models predicted damage occurrence or test their results with independent data,
565 which makes the comparison to our results difficult. Several recent studies have shown good
566 performance of RF for modelling storm disturbances (Albrecht et al., 2019; Hart et al., 2019;
567 Kabir et al., 2018). RF is a tree-based ensemble method that has similarities to BRT in the
568 aspect that it also combines a large number of regression trees in order to create accurate
569 predictions. Yet, in our results BRT did not lead to better predictive performance in cross-
570 validation or with test data compared to the two other tested methods.

571 The comparison to the studies finding good results with RF is complicated due to the
572 differences between the methods, even if they have also similarities. Our analysis differs
573 also from that of (Albrecht et al., 2019; Hart et al., 2019; Kabir et al., 2018) on a few other
574 aspects. First, we modelled wind damage on the level of forest stands, whereas the above

mentioned studies were operating on tree-level. Second, we were using longer term NFI damage observations whereas most others used data from specific storm events. However, the study by Albrecht et al. (2019) contained both event-specific and non-event-specific data and they found random forests to outperform GLMs in both types of data. Third, we performed the cross-validation without considering the spatial variation in the storm conditions (the damage density variable in our analysis). This was done because we did not want to use this variable in the prediction, as the final aim was to generalize the results to future damage events, where this information would not be available. It is possible that this approach is disadvantageous to the BRT.

While the above mentioned studies did find machine learning methods outperform logistic models in many ways, they also showed some positive sides of the logistic models. Most importantly, even though random forests showed superior performance when cross-validating models with data from one storm event in Hart et al. (2019), logistic models showed the highest AUC values compared to the other methods when the model was applied to another storm event, supporting the value of GLMs when generalizing the results to new storm events.

Use of GLMs has the extra benefit of being more easily communicated to the end user, and they can be easily applied to new use cases when model coefficient estimates are published. The interpretation of relationships between predictors and the response variable is more straightforward, whereas especially in BRTs very small changes in e.g. tree height can lead to drastic changes in model prediction (Fig. 4). The unexpectedly high damage probability values in northern Finland also demonstrate the unpredictability of BRT model behaviour. This aspect is particularly important when the end product is meant to be used in practical applications.

4.4 Applications and use of the maps

The strength of the map is in its high resolution and large extent. The high-resolution makes it useful for assessing wind damage susceptibility of individual forest stands in fragmented forest landscapes where spatial variation of forest characteristics is high. On the other hand, the national extent of the map makes it widely available and accessible to everyone who is making forest management decisions in Finnish forests. To further improve the accessibility and usability of the map, we created an openly available web map application, where users can explore the map and find the estimated wind damage vulnerabilities of the forests they are interested in, without expert knowledge in GIS software (see https://metsainfo.luke.fi/en/tuulituhoriskikartta, currently only in Finnish, click “Tuulituhoriskit” to see the wind damage vulnerability map). By providing an effective tool for identifying the vulnerable stands and for communicating wind damage risks to forest managers and owners, the map has potential to steer forest management practices towards a more disturbance-aware direction.

In addition to forest management, high-resolution information about forest wind vulnerability is crucially needed also in other sectors and applications. For example, the map can help in identifying high-risk locations where windthrown trees can harm infrastructure by damaging power lines and blocking roads. Insurance companies may also use high-resolution vulnerability information for a more risk-based pricing of forest insurances.

While wind disturbances have major consequences from the human point of view, they are a natural process and have an important role in shaping the structure and function of forest ecosystems (Bouget and Duelli, 2004; Kuuluvainen, 2002). By exploring the drivers and spatial variability of wind disturbance dynamics, our results can therefore provide insight in current disturbance regime and its effects in the ecosystem, such as biodiversity and carbon cycling. Improved information about forest disturbances and tree mortality is also urgently needed for vegetation models from stand to global scales to understand how forests will react to the changing climate (Bugmann et al., 2019; Friend et al., 2014).

When applying the map in practice, it is important to consider its limitations. First, the damage probabilities in the map are in reference to the damage happened during the study period. The amount of wind damage varies strongly between years and future conditions are not likely to exactly match the conditions during the period from which the data comes from. Therefore, instead of exact probability values, it is better to interpret the map values as relative differences in damage vulnerability. Second, it is important to note that the damage probabilities do not only refer to complete damage of the stand, as our analysis also included less severe damage cases and we did not account for damage severity. Third, it is good to keep in mind that the map presents forest vulnerability to wind and it is not possible to predict the exact location of future wind disturbances, as there are many things - such as tracks and meteorological conditions of future storms - that cannot be accounted for in the map. The uncertainties need to be taken into consideration when using the map.

Wind disturbances are strongly linked to other processes of the forest and, therefore, should be considered in larger context. Thus, the greatest benefits of our results can perhaps be achieved by combining them with information and understanding of other processes that control forest ecosystems and forest management decisions. For example, the risk model can be coupled with forest growth simulators and thereafter storm damage risks of different forest management strategies can be evaluated simultaneously when making future scenarios of forests. The map can be combined with spatial information of wood volumes and prices to assess economic risks wind disturbances. Combining wind disturbance results with the dynamics of other disturbance agents is also crucial, as wind damage is strongly linked to bark beetle outbreaks and root rot, and these interactions are becoming increasingly important with the changing climate (Seidl et al., 2017; Seidl and Rammer, 2017). A comprehensive approach is therefore needed to understand and effectively manage wind disturbances in forests.

5. Conclusions

In this study, we show how damage probability models based on NFI damage observations combined with existing spatial datasets can be used to provide a fine-scale large-extent map of wind disturbance probability. We also demonstrate the ability of the map to identify vulnerable stands in future events with an extensive external test data. These maps provide a powerful tool for supporting disturbance-aware management decisions, communicating disturbance risks to forest owners, and accounting for the effects of windthrown trees in other sectors, such as maintenance of powerline infrastructures.

Our results show that more flexible methods, such as GAM and BRT, do not always provide superior results compared to parametric statistical models, such as GLM. As the interpretation of these methods can be less straightforward, they can sometimes lead to unpredictable prediction outcomes. Therefore, it is crucial to always assess the benefits of different approaches and to carefully test the performance of the used method with test data that is not used in model fitting. Partial dependence plots and other ways for exploration of model predictions in different situations also provide useful tools for assessing if model behaviour is realistic and biologically plausible.

The success of our results is based on large and representative model data as well as high-quality and high-resolution GIS data used as map inputs. In Finland, good data sets for both the model fitting and the map inputs are available, which provided a good starting point for the work done in this study. Even though the study here was conducted for Finland, the results have high international relevance, showing that in spite of the inherent stochasticity of the wind and damage phenomena at all spatial scales, wind damage can be modelled with good accuracy across large spatial scales when existing ground and earth observation data sources are combined smartly. With improving data quality and availability (for both damage observations for model fitting and GIS data for map inputs), similar work can be extended to other regions and to other disturbance types.

Acknowledgements

678 The research was co-funded by the Finnish Forest Foundation (project MyrskyPuu). We
679 thank Ari Venäläinen and Mikko Laapas from the Finnish Meteorological Institute for their
680 advice and the maximum wind speed 10-year return level data, and the MyrskyPuu project
681 steering group (Liisa Mäkijärvi, Erno Järvinen, Heli Peltola, Ari Venäläinen and Eero Mikkola)
682 for the discussions and their insights on the topic. We also thank Kari T. Korhonen for his
683 comments on the manuscript and the whole NFI team in Luke for the NFI data we were able
684 to use in the study. We acknowledge CSC – IT Center for Science, Finland, for
685 computational resources.

References

Aalto, J., Pirinen, P., Jylhä, K., 2016. New gridded daily climatology of Finland: Permutation-based uncertainty estimates and temporal trends in climate. J. Geophys. Res. Atmospheres 121, 3807–3823. https://doi.org/10.1002/2015JD024651

Albrecht, A.T., Jung, C., Schindler, D., 2019. Improving empirical storm damage models by coupling with high-resolution gust speed data. Agric. For. Meteorol. 268, 23–31. https://doi.org/10.1016/j.agrformet.2018.12.017

Andersson, E., Keskitalo, E.C.H., Bergstén, S., 2018. In the eye of the storm: adaptation logics of forest owners in management and planning in Swedish areas. Scand. J. For. Res. 33, 800–808. https://doi.org/10.1080/02827581.2018.1494305

Bates, D., Mächler, M., Bolker, B., Walker, S., 2015. Fitting Linear Mixed-Effects Models Using lme4. J. Stat. Softw. 67, 1–48. https://doi.org/10.18637/jss.v067.i01

Bouget, C., Duelli, P., 2004. The effects of windthrow on forest insect communities: a literature review. Biol. Conserv. 118, 281–299. https://doi.org/10.1016/j.biocon.2003.09.009

Bugmann, H., Seidl, R., Hartig, F., Bohn, F., Brůna, J., Cailleret, M., François, L., Heinke, J., Henrot, A.-J., Hickler, T., Hülsmann, L., Huth, A., Jacquemin, I., Kollas, C., Lasch-Born, P., Lexer, M.J., Merganič, J., Merganičová, K., Mette, T., Miranda, B.R., Nadal-Sala, D., Rammer, W., Rammig, A., Reineking, B., Roedig, E., Sabaté, S., Steinkamp, J., Suckow, F., Vacchiano, G., Wild, J., Xu, C., Reyer, C.P.O., 2019. Tree mortality submodels drive simulated long-term forest dynamics: assessing 15 models from the stand to global scale. Ecosphere 10, e02616. https://doi.org/10.1002/ecs2.2616

Díaz-Yáñez, O., Mola_Yudego, M., González-Olabarria, J.B. (2019). Modelling damage occurrence by snow and wind in forest ecosystems. *Ecological Modelling* 408, 108741.

Dobbertin, M., 2002. Influence of stand structure and site factors on wind damage comparing

the storms Vivian and Lothar. For. Snow Landsc. Res. 77, 187–205.

Elith, J., Graham, C.H., Anderson, R.P. Dudík, M., Ferrier, S., Guisan, A., Hijmans, R.J., Huettmann, F., Leathwick, J.R., Lehmann, A., Li, J., Lohmann, L.G., Loiselle, B.A., Manion, G., Moritz, C., Nakamura, M., Nakazawa, Y., Overton, J.M.M., Peterson, A.T., Phillips, S.J., Richardson, K., Scachetti-Pereira, R., Schapire, R.E., Soberón, J., Williams, S., Wisz, M.S., Zimmermann, N.E., 2006. Novel methods improve prediction of species' distributions from occurrence data. Ecography 29, 129–151.

Elith, J., Leathwick, J.R., Hastie, T., 2008. A working guide to boosted regression trees. J. Anim. Ecol. 77, 802–813. https://doi.org/10.1111/j.1365-2656.2008.01390.x

Fox, J., Monette, G., 1992. Generalized Collinearity Diagnostics. J. Am. Stat. Assoc. 87, 178–183. https://doi.org/10.1080/01621459.1992.10475190

Fridman, J., Valinger, E., 1998. Modelling probability of snow and wind damage using tree, stand, and site characteristics from Pinus sylvestris sample plots. Scand. J. For. Res. 13, 348–356. https://doi.org/10.1080/02827589809382994

Friend, A.D., Lucht, W., Rademacher, T.T., Keribin, R., Betts, R., Cadule, P., Ciais, P., Clark, D.B., Dankers, R., Falloon, P.D., Ito, A., Kahana, R., Kleidon, A., Lomas, M.R., Nishina, K., Ostberg, S., Pavlick, R., Peylin, P., Schaphoff, S., Vuichard, N., Warszawski, L., Wiltshire, A., Woodward, F.I., 2014. Carbon residence time dominates uncertainty in terrestrial vegetation responses to future climate and atmospheric CO2. Proc. Natl. Acad. Sci. 111, 3280–3285. https://doi.org/10.1073/pnas.1222477110

Gregow, H., Laaksonen, A., Alper, M.E., 2017. Increasing large scale windstorm damage in Western, Central and Northern European forests, 1951–2010. Sci. Rep. 7, 46397. https://doi.org/10.1038/srep46397

Gregow, H., Peltola, H., Laapas, M., Saku, S., Venäläinen, A., 2011. Combined occurrence of wind, snow loading and soil frost with implications for risks to forestry in Finland under the current and changing climatic conditions. Silva Fenn. 45. https://doi.org/10.14214/sf.30

GTK, 2018. Superficial deposits of Finland 1:200 000 (sediment polygons). http://tupa.gtk.fi/paikkatieto/meta/maapera_200k.html (accessed 4.29.19).

Hanewinkel, M., Zhou, W., Schill, C., 2004. A neural network approach to identify forest stands susceptible to wind damage. For. Ecol. Manag. 196, 227–243. https://doi.org/10.1016/j.foreco.2004.02.056

Hart, E., Sim, K., Kamimura, K., Meredieu, C., Guyon, D., Gardiner, B., 2019. Use of machine learning techniques to model wind damage to forests. Agric. For. Meteorol. 265, 16–29. https://doi.org/10.1016/j.agrformet.2018.10.022

Hastie, T., Tibshirani, R., Friedman, J., 2009. The elements of statistical learning, 2nd ed, Springer Series in Statistics. Springer-Verlag New York.

Hijmans, R.J., 2017. raster: Geographic Data Analysis and Modeling. R package version 2.6-7. https://CRAN.R-project.org/package=raster.

Hijmans, R.J., Phillips, S., Leathwick, J., Elith, J., 2017. dismo: Species Distribution Modeling. R package version 1.1-4. https://CRAN.R-project.org/package=dismo.

Honkaniemi, J., Lehtonen, M., Väisänen, H., Peltola, H., 2017. Effects of wood decay by Heterobasidion annosum on the vulnerability of Norway spruce stands to wind damage: a mechanistic modelling approach. Can. J. For. Res. 47, 777–787. https://doi.org/10.1139/cjfr-2016-0505

Hosmer, D.W., Lemeshow, S., Strudivant, R.X., 2013. Applied Logistic Regression, 3rd ed. John Wiley & Sons, New York.

Ikonen, V.-P., Kilpeläinen, A., Zubizarreta-Gerendiain, A., Strandman, H., Asikainen, A., Venäläinen, A., Kaurola, J., Kangas, J., Peltola, H., 2017. Regional risks of wind damage in boreal forests under changing management and climate projections. Can. J. For. Res. 47, 1632–1645. https://doi.org/10.1139/cjfr-2017-0183

Kabir, E., Guikema, S., Kane, B., 2018. Statistical modeling of tree failures during storms. Reliab. Eng. Syst. Saf. 177, 68–79. https://doi.org/10.1016/j.ress.2018.04.026

Kamimura, K., Gardiner, B., Dupont, S., Guyon, D., Meredieu, C., 2015. Mechanistic and statistical approaches to predicting wind damage to individual maritime pine (Pinus

pinaster) trees in forests. Can. J. For. Res. 46, 88–100. https://doi.org/10.1139/cjfr-2015-0237

Korhonen, K.T., 2016. National forest inventories : Assessment of wood availability and use : Finland, in: Vidal, C., Alberdi, I., Hernández, L., Redmond, J.J. (Eds.), National Forest Inventories : Assessment of Wood Availability and Use. Springer International Publishing, Switzerland, pp. 369–384.

Korhonen, K.T., Ihalainen, A., Ahola, A., Heikkinen, J., Henttonen, H.M., Hotanen, J.-P., Nevalainen, S., Pitkänen, J., Strandström, M., Viiri, H., 2017. Suomen metsät 2009–2013 ja niiden kehitys 1921–2013 (No. 59/2017), Luonnonvara- ja biotalouden tutkimus. Natural Resources Institute Finland (Luke).

Kufeoglu, S., Lehtonen, M. (2014). Cyclone Dagmar of 2011 and its impacts in Finland. 5th IEEE PES Innovative Smart Grid Technologies Europe (ISGT Europe), October 12-15, Istanbul.

Kuuluvainen, T., 2002. Disturbance dynamics in boreal forests: defining the ecological basis of restoration and management of biodiversity. Silva Fenn. 36, 5–11.

Laapas, M., Lehtonen, I., Venäläinen, A., Peltola, H.M., 2019. The 10-Year Return Levels of Maximum Wind Speeds under Frozen and Unfrozen Soil Forest Conditions in Finland. Climate 7, 62. https://doi.org/10.3390/cli7050062

Lanquaye-Opoku, N., Mitchell, S.J., 2005. Portability of stand-level empirical windthrow risk models. For. Ecol. Manag. 216, 134–148. https://doi.org/10.1016/j.foreco.2005.05.032

Lohmander, P., Helles, F., 1987. Windthrow probability as a function of stand characteristics and shelter. Scand. J. For. Res. 2, 227–238. https://doi.org/10.1080/02827588709382460

Mäkisara, K., Katila, M., Peräsaari, J., 2019. The Multi-Source National Forest Inventory of Finland - methods and results 2015 (No. 8/2019), Natural Resources and Bioeconomy Studies. Natural Resources Institute Finland (Luke).

Mäkisara, K., Katila, M., Tomppo, E., 2016. The Multi-Source National Forest Inventory of

798 Finland – methods and results 2013 (No. 10/2016), Natural Resources and
799 Bioeconomy Studies. Natural Resources Institute Finland (Luke).
800 Mattila, U., Nuutinen, T., 2007. Assessing the incidence of butt rot in Norway spruce in
801 southern Finland. Silva Fenn. 41. https://doi.org/10.14214/sf.473
802 Mitchell, S.J., 2013. Wind as a natural disturbance agent in forests: a synthesis. For. Int. J.
803 For. Res. 86, 147–157. https://doi.org/10.1093/forestry/cps058
804 Müller, M.M., Henttonen, H.M., Penttilä, R., Kulju, M., Helo, T., Kaitera, J., 2018. Distribution
805 of Heterobasidion butt rot in northern Finland. For. Ecol. Manag. 425, 85–91.
806 https://doi.org/10.1016/j.foreco.2018.05.047
807 Nakou, A., Sauter, U.H., Kohnle, U., 2016. Improved models of harvest-induced bark
808 damage. Ann. For. Sci. 73, 233–246. https://doi.org/10.1007/s13595-015-0530-5
809 Narendra, P.M., Goldberg, M., 1980. Image Segmentation with Directed Trees. IEEE Trans.
810 Pattern Anal. Mach. Intell. PAMI-2, 185–191.
811 https://doi.org/10.1109/TPAMI.1980.4766999
812 Nicoll, B.C., Gardiner, B.A., Rayner, B., Peace, A.J., 2006. Anchorage of coniferous trees in
813 relation to species, soil type, and rooting depth. Can. J. For. Res. 36, 1871–1883.
814 NLS, 2018. Topographic Database https://www.maanmittauslaitos.fi/en/maps-and-spatial-
815 data/expert-users/product-descriptions/topographic-database.
816 Pebesma, E.J., Bivand, R.S., 2005. Classes and methods for spatial data in R (No. 5 (2),
817 https://cran.r-project.org/doc/Rnews/), R News.
818 Pekkarinen, A., 2002. Image segment-based spectral features in the estimation of timber
819 volume. Remote Sens. Environ. 82, 349–359. https://doi.org/10.1016/S0034-
820 4257(02)00052-4
821 Peltola, H., Ikonen, V.-P., Gregow, H., Strandman, H., Kilpeläinen, A., Venäläinen, A.,
822 Kellomäki, S., 2010. Impacts of climate change on timber production and regional
823 risks of wind-induced damage to forests in Finland. For. Ecol. Manag. 260, 833–845.
824 https://doi.org/10.1016/j.foreco.2010.06.001
825 Peltola, H., Kellomäki, S., Väisänen, H., Ikonen, V.-P., 1999. A mechanistic model for

826 assessing the risk of wind and snow damage to single trees and stands of Scots
827 pine, Norway spruce, and birch. Can. J. For. Res. 29, 647–661.
828 https://doi.org/10.1139/x99-029
829 R Core Team, 2018. R: A language and environment for statistical computing. R Foundation
830 for Statistical Computing, Vienna, Austria. https://www.R-project.org/.
831 Reyer, C.P.O., Bathgate, S., Blennow, K., Borges, J.G., Bugmann, H., Delzon, S., Faias,
832 S.P., Garcia-Gonzalo, J., Gardiner, B., Gonzalez-Olabarria, J.R., Gracia, C.,
833 Hernández, J.G., Kellomäki, S., Kramer, K., Lexer, M.J., Lindner, M., Maaten, E. van
834 der, Maroschek, M., Muys, B., Nicoll, B., Palahi, M., Palma, J.H., Paulo, J.A., Peltola,
835 H., Pukkala, T., Rammer, W., Ray, D., Sabaté, S., Schelhaas, M.-J., Seidl, R.,
836 Temperli, C., Tomé, M., Yousefpour, R., Zimmermann, N.E., Hanewinkel, M., 2017.
837 Are forest disturbances amplifying or canceling out climate change-induced
838 productivity changes in European forests? Environ. Res. Lett. 12, 034027.
839 https://doi.org/10.1088/1748-9326/aa5ef1
840 Robin, X., Turck, N., Hainard, A., Tiberti, N., Lisacek, F., Sanchez, J.-C., Müller, M., 2011.
841 pROC: an open-source package for R and S+ to analyze and compare ROC curves.
842 BMC Bioinformatics 12, 77. https://doi.org/10.1186/1471-2105-12-77
843 Saarinen, N., Vastaranta, M., Honkavaara, E., Wulder, M.A., White, J.C., Litkey, P.,
844 Holopainen, M., Hyyppä, J., 2016. Using multi-source data to map and model the
845 predisposition of forests to wind disturbance. Scand. J. For. Res. 31, 66–79.
846 https://doi.org/10.1080/02827581.2015.1056751
847 Schelhaas, M.-J., Nabuurs, G.-J., Schuck, A., 2003. Natural disturbances in the European
848 forests in the 19th and 20th centuries. Glob. Change Biol. 9, 1620–1633.
849 https://doi.org/10.1046/j.1365-2486.2003.00684.x
850 Schindler, D., Grebhan, K., Albrecht, A., Schönborn, J., 2009. Modelling the wind damage
851 probability in forests in Southwestern Germany for the 1999 winter storm ‘Lothar.’ Int.
852 J. Biometeorol. 53, 543–554. https://doi.org/10.1007/s00484-009-0242-3
853 Schindler, D., Jung, C., Buchholz, A., 2016. Using highly resolved maximum gust speed as

predictor for forest storm damage caused by the high-impact winter storm Lothar in Southwest Germany. Atmospheric Sci. Lett. 17, 462–469. https://doi.org/10.1002/asl.679

Schmidt, M., Hanewinkel, M., Kändler, G., Kublin, E., Kohnle, U., 2010. An inventory-based approach for modeling single-tree storm damage — experiences with the winter storm of 1999 in southwestern Germany. Can. J. For. Res. 40, 1636–1652. https://doi.org/10.1139/X10-099

Seidl, R., Rammer, W., 2017. Climate change amplifies the interactions between wind and bark beetle disturbances in forest landscapes. Landsc. Ecol. 32, 1485–1498. https://doi.org/10.1007/s10980-016-0396-4

Seidl, R., Schelhaas, M.-J., Lexer, M.J., 2011. Unraveling the drivers of intensifying forest disturbance regimes in Europe. Glob. Change Biol. 17, 2842–2852. https://doi.org/10.1111/j.1365-2486.2011.02452.x

Seidl, R., Schelhaas, M.-J., Rammer, W., Verkerk, P.J., 2014. Increasing forest disturbances in Europe and their impact on carbon storage. Nat. Clim. Change 4, 806–810. https://doi.org/10.1038/nclimate2318

Seidl, R., Thom, D., Kautz, M., Martin-Benito, D., Peltoniemi, M., Vacchiano, G., Wild, J., Ascoli, D., Petr, M., Honkaniemi, J., Lexer, M.J., Trotsiuk, V., Mairota, P., Svoboda, M., Fabrika, M., Nagel, T.A., Reyer, C.P.O., 2017. Forest disturbances under climate change. Nat. Clim. Change 7, 395–402. https://doi.org/10.1038/nclimate3303

Suvanto, S., Henttonen, H.M., Nöjd, P., Mäkinen, H., 2018. High-resolution topographical information improves tree-level storm damage models. Can. J. For. Res. 48, 721–728. https://doi.org/10.1139/cjfr-2017-0315

Suvanto, S., Henttonen, H.M., Nöjd, P., Mäkinen, H., 2016. Forest susceptibility to storm damage is affected by similar factors regardless of storm type: Comparison of thunder storms and autumn extra-tropical cyclones in Finland. For. Ecol. Manag. 381, 17–28. https://doi.org/10.1016/j.foreco.2016.09.005

Tomppo, E., Haakana, M., Katila, M., Peräsaari, J., 2008. Multi-Source National Forest

Inventory: Methods and Applications, Managing Forest Ecosystems. Springer Netherlands.

Tomppo, E., Heikkinen, J., Henttonen, H.M., Ihalainen, A., Katila, M., Mäkelä, H., Tuomainen, T., Vainikainen, N., 2011. Designing and Conducting a Forest Inventory - case: 9th National Forest Inventory of Finland, Managing Forest Ecosystems. Springer Netherlands.

Valinger, E., Fridman, J., 2011. Factors affecting the probability of windthrow at stand level as a result of Gudrun winter storm in southern Sweden. For. Ecol. Manag. 262, 398–403. https://doi.org/10.1016/j.foreco.2011.04.004

Valinger, E., Fridman, J., 1997. Modelling probability of snow and wind damage in Scots pine stands using tree characteristics. For. Ecol. Manag. 97, 215–222. https://doi.org/10.1016/S0378-1127(97)00062-5

Valinger, E., Kempe, G., Fridman, J., 2014. Forest management and forest state in southern Sweden before and after the impact of storm Gudrun in the winter of 2005. Scand. J. For. Res. 29, 466–472. https://doi.org/10.1080/02827581.2014.927528

Venäläinen, A., Laapas, M., Pirinen, P., Horttanainen, M., Hyvönen, R., Lehtonen, I., Junila, P., Hou, M., Peltola, H.M., 2017. Estimation of the high-spatial-resolution variability in extreme wind speeds for forestry applications. Earth Syst. Dyn. 8, 529–545. https://doi.org/10.5194/esd-8-529-2017

Viiri, H., Ahola, A., Ihalainen, A., Korhonen, K.T., Muinonen, E., Parikka, H., Pitkänen, J., 2011. Kesän 2010 myrskytuhot ja niistä seuraava hyönteistuhoriski (In Finnish). *Metsätieteen aikakauskirja* 3, 221–225.

Wallentin, C., Nilsson, U., 2014. Storm and snow damage in a Norway spruce thinning experiment in southern Sweden. For. Int. J. For. Res. 87, 229–238. https://doi.org/10.1093/forestry/cpt046

Wand, M., 2015. KernSmooth: Functions for Kernel Smoothing Supporting Wand & Jones (1995), R package version 2.23-15. https://CRAN.R-project.org/package=KernSmooth.

910 Wood, S., 2017. Generalized Additive Models: An Introduction with R, Second Edition, 2nd
911 edition. ed.
912 Wood, S.N., 2011. Fast stable restricted maximum likelihood and marginal likelihood
913 estimation of semiparametric generalized linear models. J. R. Stat. Soc. Ser. B Stat.
914 Methodol. 73, 3–36.
915 Wood, S.N., Scheipl, F., 2017. gamm4: Generalized Additive Mixed Models using “mgcv”
916 and “lme4”. R package version 0.2-5. https://CRAN.R-project.org/package=gamm4.
917

Tables

Table 1. Description of predictors used and their sources in the model and in the damage probability map. See section 2.2.1 for details. Abbreviations: NFI11 – 11th Finnish National Forest Inventory, NFI12 – 12th Finnish National Forest Inventory, MS-NFI – multi-source NFI, GTK – Geological Survey of Finland, NLS – National Land Survey of Finland.

Variable	Type*	Unit / Classes	Source in model	Source in map
Tree species	C	pine, spruce, other	NFI11	MS-NFI 2015
Tree height	N	dm	NFI11	MS-NFI 2015
Time since thinning	C	0-5, 6-10, > 10 years	NFI11	MS-NFI 2015, Forest use notifications
Wind (10-year return level of max wind speed)	N	ms^{-1}	Venäläinen et al. 2017	Venäläinen et al. 2017
Open neighbor stand	C	True, False	MS-NFI 2013	MS-NFI 2015
Soil type	C	Mineral/coarse, Mineral/fine, Organic	NFI11	GTK 2018, NLS 2018
Mineral soil depth < 30 cm	C	True, False	NFI11	GTK 2018, NLS 2018
Site fertility	C	Fertile, Poor	NFI11	MS-NFI 2015
Temperature sum (average 1985-2014)	N	100 dd (over 5C)	Aalto et al. 2016	Aalto et al. 2016
Damage density ratio	C	0-2, 2-3, <3	NFI11	In the calculation of the map, this variable was included as a weighted average of all classes, because it was included in the model only to account for spatial structures in storm severity.

** C – categorical, N – numerical (continuous)*

924 **Table 2.** Descriptive statistics for the NFI11 data. Mean and standard deviation for non-
925 damaged, damaged and all plots continuous variables, and percentages of each class for
926 categorical variables. The definitions of the variables are in table 1.

	Non-damaged	Damaged	All
Number of plots	40322	1070	41392
Species			
Scots pine	63.4%	59.1%	63.3%
Norway spruce	24.0%	36.8%	24.3%
Other	12.6%	4.1%	12.4%
Tree height	163.0 (50.5)	195.2 (45.1)	163.9 (50.6)
Time since thinning			
0-5 years	13.4%	26.0%	13.7%
6-10 years	9.2%	15.5%	9.4%
> 10 years	77.4%	58.5%	76.9%
Wind	12.1 (2.0)	12.5 (2.0)	12.2 (2.0)
Open neighbor			
False	85.7%	84.6%	85.7%
True	14.3%	15.4%	14.3%
Soil type			
Mineral, coarse	66.9%	77.8%	67.2%
Mineral, fine	12.7%	9.8%	12.7%
Organic	20.3%	12.4%	20.1%
Soil depth < 30 cm			
False	89.5%	85.0%	89.4%
True	10.5%	15.0%	10.6%
Site fertility			
Poor	34.8%	31.9%	34.7%
Fertile	65.2%	68.1%	65.3%
Temperature sum	1,185 (178.9)	1,262.6 (130.4)	1,187.0 (178.3)

927

928 **Table 3.** GLM model results. See Table 1 for descriptions of variables. For categorical
929 variables, the first class listed in Table 1 is the reference class and not listed separately in
930 this table, i.e., the results of other classes are presented in reference to the reference class.
931 Classes of categorical variables are presented as subscripts. Colons are used to present
932 interaction terms between variables.

	Estimate	Std. Error	z value	Pr(>|z|)
(Intercept)	-14.690	1.061	-13.841	< 0.001
$Species_{Spruce}$	-8.494	1.918	-4.430	< 0.001
$Species_{Other}$	-9.314	3.931	-2.370	0.018
log(Height)	1.661	0.189	8.807	< 0.001
$Last\ thinning_{6\text{-}10\ years}$	-0.298	0.113	-2.637	0.008
$Last\ thinning_{over\ 10\ years}$	-0.844	0.084	-9.995	< 0.001
log(Wind)	0.749	0.238	3.152	0.002
$Open\ stand\ border_{TRUE}$	0.310	0.095	3.284	0.001
$Soil_{mineral,\ fine}$	-0.356	0.124	-2.875	0.004
$Soil_{organic}$	-0.216	0.110	-1.962	0.050
$Soil\ depth < 30cm_{TRUE}$	0.214	0.106	2.011	0.044
$Site\ fertility_{Fertile}$	-0.425	0.092	-4.611	< 0.001
Temperature sum	0.096	0.025	3.843	< 0.001
$Damage\ density_{2\text{-}3}$	1.104	0.088	12.498	< 0.001
$Damage\ density_{>3}$	1.898	0.111	17.137	< 0.001
$Species_{Spruce}$: log(Height)	1.634	0.358	4.561	< 0.001
$Species_{Other}$: log(Height)	1.625	0.742	2.190	0.029

933
934

Figures

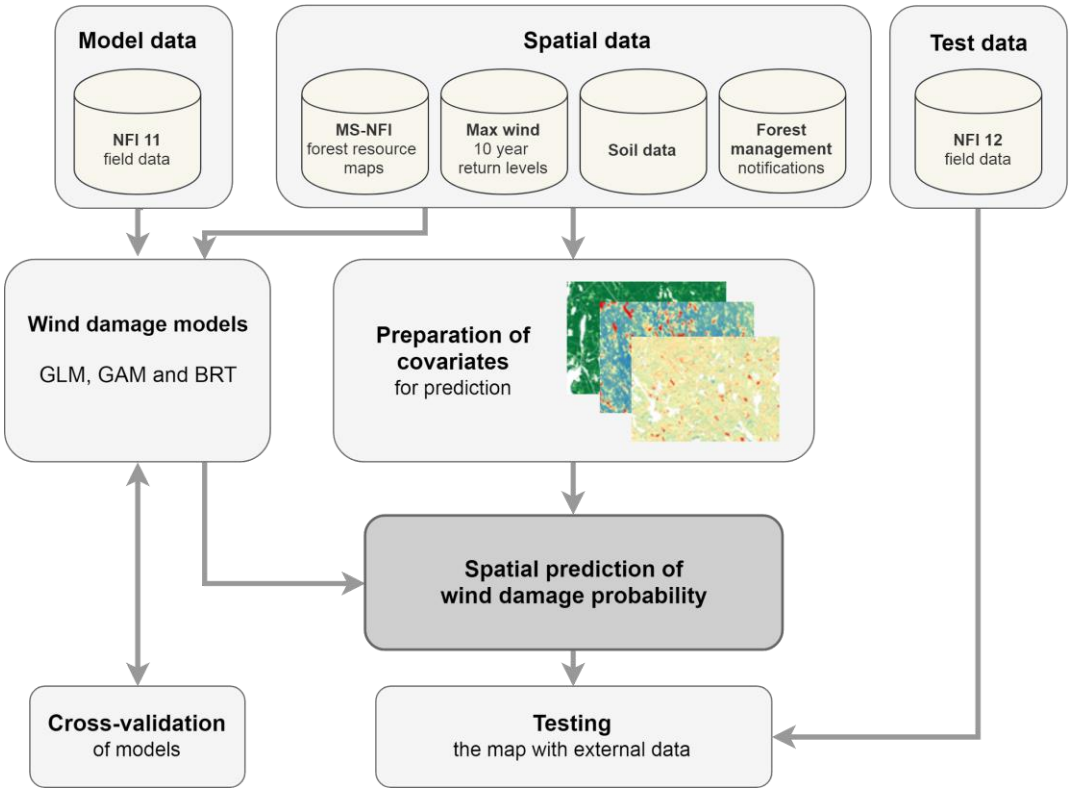

Figure 1. General approach and workflow. Abbreviations in the figure: NFI – national forest inventory, MS-NFI – multi-source national forest inventory, GLM – generalized linear model, GAM – generalized additive model, BRT – boosted regression trees

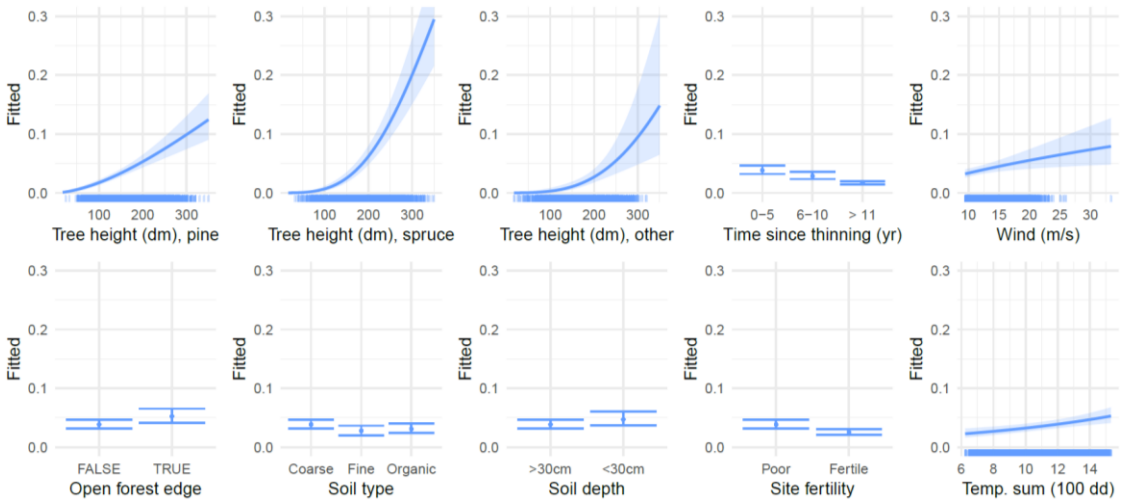

941

942 **Figure 2.** GLM partial dependence plots for the map predictors. Prediction of damage
943 probability is calculated for the range of each predictor variable when other predictors are set
944 to average (continuous variables) or reference class (categorical variables). Rugged x-axis
945 describes the distribution of data. Confidence intervals are calculated as 2 x prediction
946 standard error (in the scale of the linear predictor).

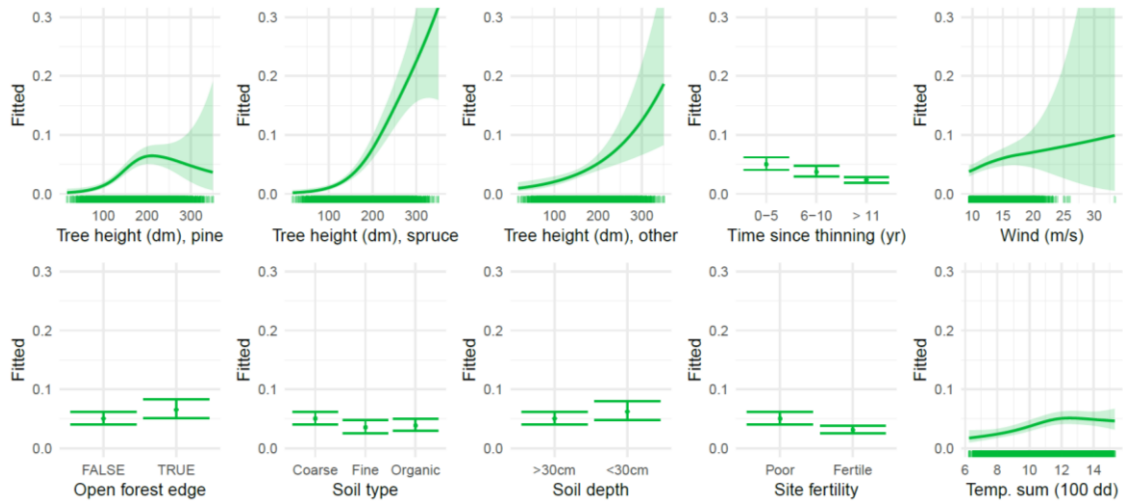

947

948 **Figure 3.** GAM partial dependence plots for the map predictors. Prediction of damage
949 probability is calculated for the range of each predictor variable when other predictors are set
950 to average (continuous variables) or reference class (categorical variables). Rugged x-axis
951 describes the distribution of data. Confidence intervals are calculated as 2 x prediction
952 standard error (in the scale of the linear predictor).

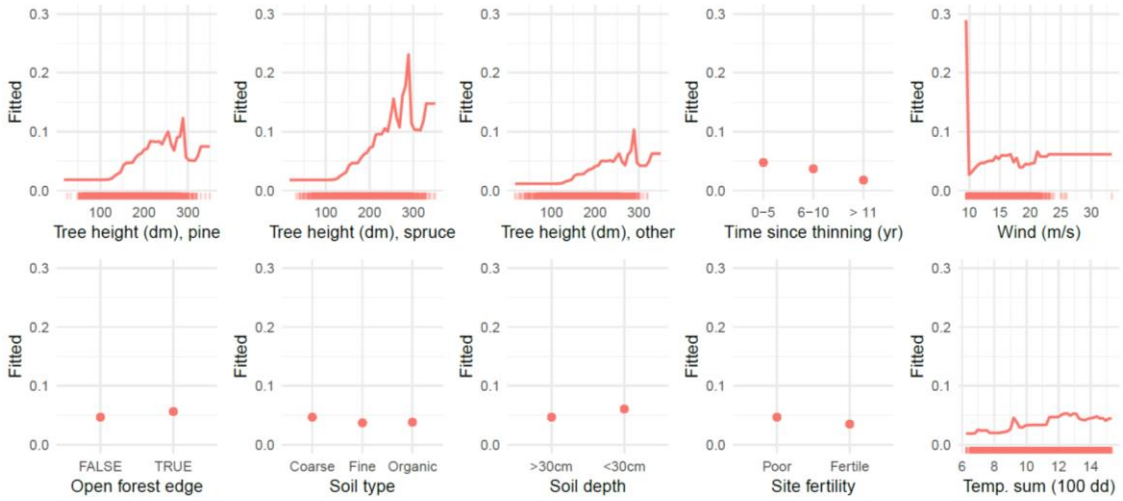

953

954 **Figure 4.** BRT partial dependence plots for the map predictors. Prediction of damage
955 probability is calculated for the range of each predictor variable when other predictors are set
956 to average (continuous variables) or reference class (categorical variables). Rugged x-axis
957 describes the distribution of data.

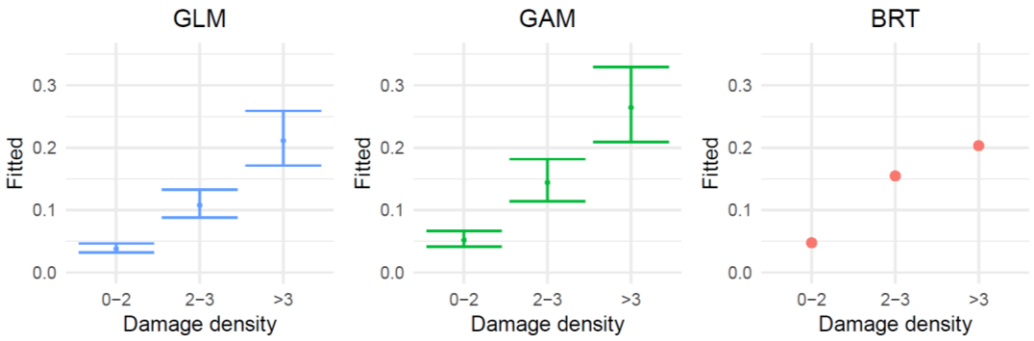

958

959 **Figure 5.** Partial dependence plots for damage density in the different models (GLM, GAM
960 and BRT). Damage density was included in the models to account for spatial variation in
961 severity of storm damage in the data, and it was set to 0 when calculating the wind damage
962 probability map. Note that the y-axis range differs from figures 2-4.

963

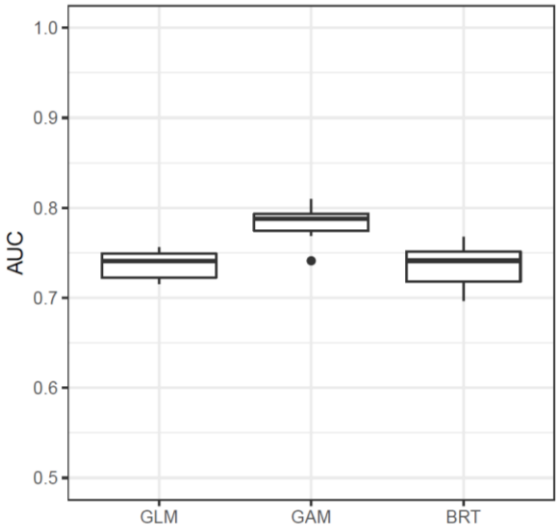

964

965 **Figure 6.** Distribution of AUC values in the 10-fold cross-validation for GLM, GAM and BRT.

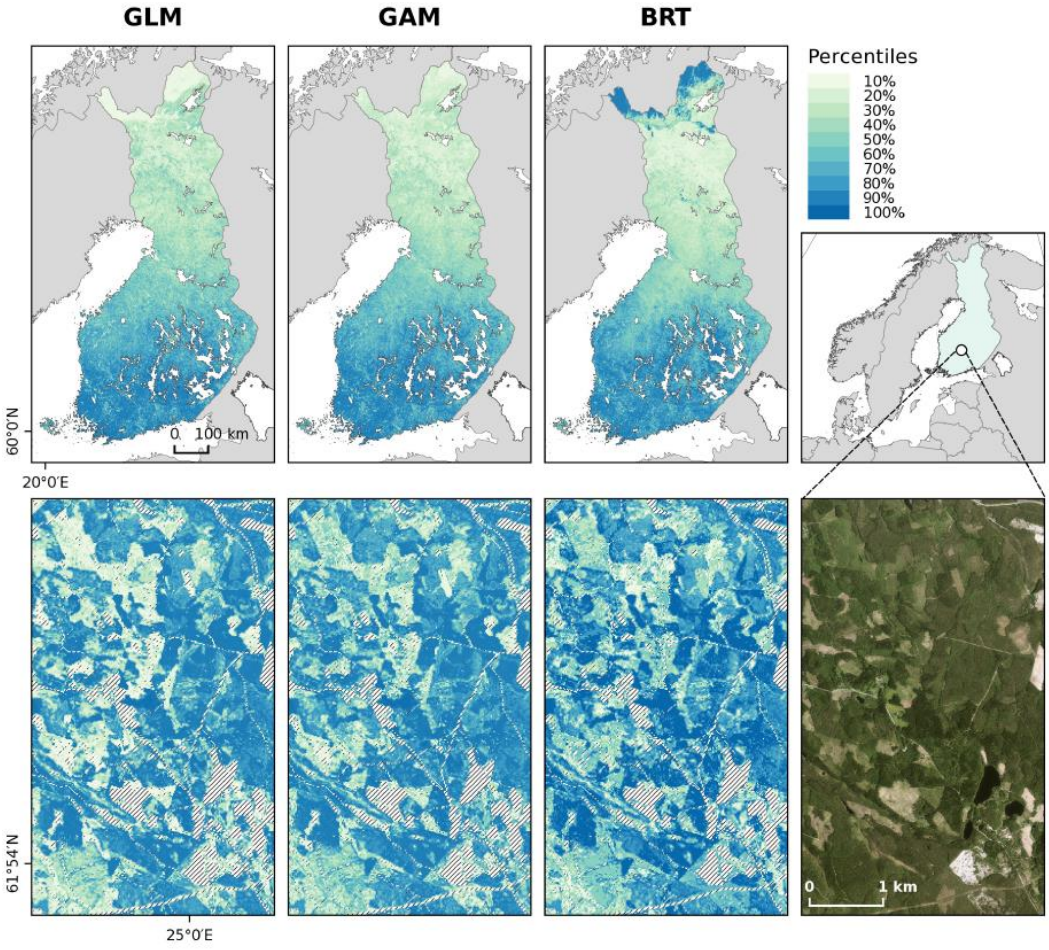

966

967 **Figure 7.** Damage vulnerability maps calculated for the whole country (upper panel) and a

968 fine-scale detail of the maps (lower panel), calculated with the three different damage

probability models (GLM, GAM and BRT), and an orthophoto from the same location (B). Colors in the damage vulnerability map are defined by the percentiles of the map data (e.g., the first class contain the lowest 10% of map values). The upper panel maps are resampled to 1 km x 1 km resolution with bilinear interpolation. Note that the orthophoto is not from the exact same time as the forest resource data used for the calculation of the map. Orthophoto © National Land Survey of Finland, published under CC-BY 4.0 licence.

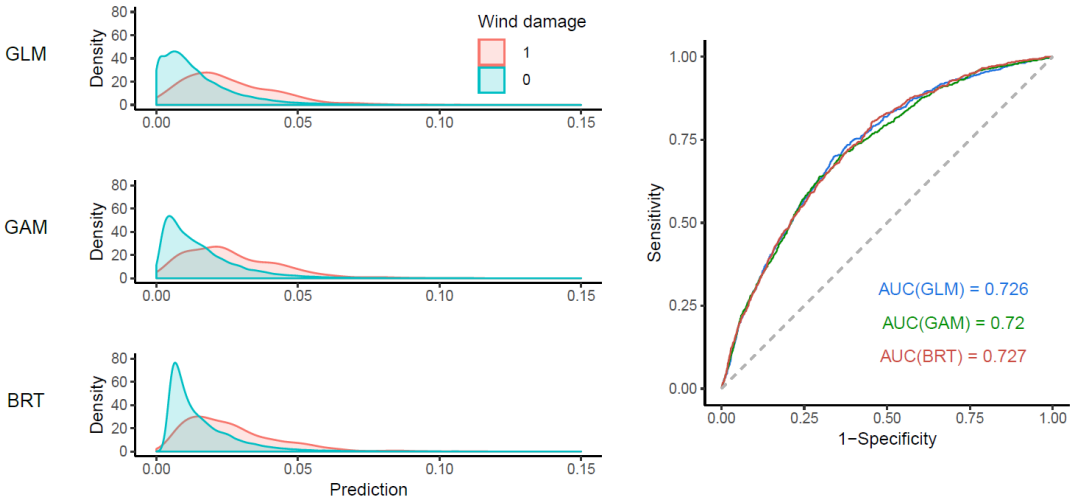

Figure 8. Density plots of the distributions of map predictions for test data plots with wind damage (red) and without wind damage (blue), and ROC curve showing the ability of the maps to distinguish between damaged and non-damaged test plots for the different model methods (GLM, GAM and BRT).

Supplementary materials

S1. The damage density ratio variable

S2. GAM model results

S3. BRT parameter tuning

S4. GLM variance-covariance matrix

S5. Maps of the model, test and predictor data sets